Optical pumping of metastable NH radicals into the paramagnetic ground state

Sebastiaan Y. T. van de Meerakker[1] Boris G. Sartakov,[2] Allard P. Mosk,[1] Rienk T. Jongma,[1] and Gerard Meijer[1,3,4]
[1]*FOM–Institute for Plasmaphysics Rijnhuizen, P.O. Box 1207, NL-3430 BE Nieuwegein, The Netherlands*
[2]*General Physics Institute RAS, Vavilov street 38, 119991 Moscow, Russia*
[3]*Department of Molecular and Laser Physics, University of Nijmegen, Toernooiveld 1, NL-6525 ED Nijmegen, The Netherlands*
[4]*Fritz-Haber-Institut der Max-Planck-Gesellschaft, Faradayweg 4-6, D-14195 Berlin, Germany*
(Received 19 May 2003; published 15 September 2003)

We here report on the optical pumping of both ^{14}NH and ^{15}NH radicals from the metastable $a\,^1\Delta$ state into the $X\,^3\Sigma^-$ ground state in a molecular beam experiment. By inducing the hitherto unobserved spin-forbidden $A\,^3\Pi \leftarrow a\,^1\Delta$ transition, followed by spontaneous emission to the $X\,^3\Sigma^-$ state, a unidirectional pathway for population transfer from the metastable state into the electronic ground state is obtained. The optical pumping scheme demonstrated here opens up the possibility to accumulate NH radicals in a magnetic or optical trap.

DOI: 10.1103/PhysRevA.68.032508 PACS number(s): 33.70.Ca, 33.80.Ps, 33.70.Fd, 33.20.Kf

I. INTRODUCTION

During the last few years a variety of experimental methods have been developed to produce translationally cold molecules [1–3]. Photoassociation of trapped alkali atoms is the method used by most research groups working in this field. Thus produced diatomic molecules can subsequently be trapped in the focus of an intense off-resonant laser beam or in a magnetic trap. Recently, a total number of 2×10^5 Cs_2 molecules at a density of about 10^7 molecules/cm^3 have been magnetically trapped at a temperature of 30 μK [4]. In another experimental approach, paramagnetic molecules that are injected into a cryogenic He cell are thermalized using multiple collisions with the He atoms. By placing the He cell at the center of an inhomogeneous magnetic field, this method of buffer-gas cooling has yielded a relatively large number of 10^8 trapped CaH molecules in a 1-cm^3 volume at a temperature of 400 mK [5]. The method developed in our laboratory makes use of a series of time-varying electric fields to repeatedly extract kinetic energy from polar molecules in a pulsed molecular beam. With this method of Stark deceleration the high phase-space density present in the moving frame of a pulsed molecular beam is transferred to the laboratory frame. The slowed beams of molecules are subsequently electrostatically trapped [6] or confined in a storage ring [7]. To date, ND_3 molecules have been trapped in a 1-mm^3 volume in a quadrupole trap at densities higher than 10^7/cm^3 and at temperatures around 25 mK [8]. These experimental advances, together with the many other experimental techniques that are currently being explored and together with the numerous theoretical predictions on the fascinating properties of dense samples of cold (polar) molecules [9], make the field of cold molecules a very active and promising field of research.

To be able to study intermolecular interactions in these cold gases, for instance, to investigate the prospects of evaporative cooling to reach quantum degeneracy, the phase-space density of the trapped molecular sample needs to be increased, i.e., the number density needs to be increased and/or the temperature needs to be reduced. Simply reloading the trap to increase the number density is not possible without losing the molecules that are already stored; the Liouville theorem dictates that dissipation is required to increase the phase-space density. Recently we proposed a scheme that circumvents this fundamental obstacle and that enables, specifically for the NH radical, reloading of a magnetic trap [10]. For this scheme, a beam of NH molecules in the long-lived metastable $a\,^1\Delta$ state needs to be produced. Molecules in this state interact strongly with electric fields and, when in the appropriate quantum levels, can be efficiently decelerated in a series of time-varying electric fields. At the point where the NH molecules have come to a near standstill, they can be optically pumped to the $X\,^3\Sigma^-$ electronic ground state by inducing the spin-forbidden $A\,^3\Pi \leftarrow a\,^1\Delta$ transition, followed by spontaneous emission in the triplet system. In this way a unidirectional pathway for population transfer of the translationally cold molecules from the metastable state into the electronic ground state can be obtained. In the ground state, the NH molecules interact strongly with magnetic fields and can be readily trapped in inhomogeneous magnetic fields; its $2\mu_B$ magnetic moment actually makes the NH radical one of the prime candidates in molecular magnetic trapping experiments. As the Stark interaction in the ground state is very weak, the electric fields of the decelerator hardly affect the magnetic trapping potential and the magnetic trap can therefore be directly superimposed with the point where the NH radicals have been electrostatically stopped. Alternatively, optical trapping can be employed near the exit of the decelerator.

There are additional features that make the NH radical an interesting system to the field of cold molecules. Two bosonic (^{15}NH,^{14}ND) and two fermionic (^{14}NH,^{15}ND) isotopomers can be produced, of which in particular ^{15}NH has a relatively simple hyperfine structure. Molecules in both the electronic ground state and in the electronically excited metastable state can be sensitively detected using laser induced fluorescence (LIF) on strong, electric dipole allowed, transitions in the ultraviolet spectral region. Moreover, the $A\,^3\Pi, v=0 \leftarrow X\,^3\Sigma^-, v=0$ transition around 336 nm has a Franck-Condon factor of better than 0.999 [11]. It should be remarked, however, that in this highly diagonal system the actual ratio of the oscillator strengths of the diagonal to the

off-diagonal transitions depends sensitively on the r dependence of the transition dipole moment. But even so, measurements indicate that the ratio of the transition probabilities of the $(v=0\rightarrow v=0)$ and the $(v=0\rightarrow v=1)$ transition is better than 99.3% [12]. As in addition a closed rotational transition can be found, this offers interesting prospects for direct laser cooling. The NH radical is also an interesting species for cold chemistry studies. NH radicals in their metastable $a\,^1\Delta$ state, which are isoelectronic with O (^{1}D) and CH_2 ($\tilde{a}\,^1A_1$) and isovalent with NF ($a\,^1\Delta$) and NCl ($a\,^1\Delta$), are regarded as a model system to study elementary reactions of electronically excited species [13].

To investigate the prospects of the proposed optical pumping scheme of the metastable NH radicals into their electronic ground state, the spin-forbidden $A\,^3\Pi\leftarrow a\,^1\Delta$ transition needs to be characterized. Although this transition has never been experimentally observed, the singlet-triplet splitting in NH is known quite well. The singlet and triplet systems of NH were first connected by the observation of the $b\,^1\Sigma^+\rightarrow X\,^3\Sigma^-$ transition [14] in emission. The most accurate value of the singlet-triplet splitting to date is derived from a direct measurement of the $a\,^1\Delta\rightarrow X\,^3\Sigma^-$ transition [15]. Based on these measurements, the $A\,^3\Pi,v=0\leftarrow a\,^1\Delta,v=0$ transition is expected around 584 nm, and can be recorded using LIF detection. For the application of NH in Stark deceleration experiments, an intense pulsed beam of metastable NH radicals is required. Although many cell experiments with NH ($a\,^1\Delta$), using a variety of production schemes, have been carried out, only a few studies have been performed with metastable NH in a molecular beam [16–19]. We here report on the successful production of a pulsed molecular beam of metastable NH ($a\,^1\Delta$) radicals using a discharge source. Efficient transfer of the molecules to the electronic ground state $X\,^3\Sigma^-$ by optical pumping via the spin-forbidden $A\,^3\Pi\leftarrow a\,^1\Delta$ transition, the most critical step in the proposed trap reloading experiments [10], is demonstrated to be possible.

II. EXPERIMENT

The experiments are performed in a molecular beam machine consisting of two differentially pumped vacuum chambers. The source chamber and detection chamber are pumped by a 1400 l/s (Pfeiffer Vacuum TMU 1600M) and a 400 l/s (TMU 400M) turbomolecular drag pump, respectively. The NH molecules are formed in an electrical discharge during the expansion of a mixture of about 1% NH_3 in He into vacuum through a commercially available pulsed supersonic valve (R.M. Jordan, Inc.). The valve has a pulse duration of approximately 40 μs and operates at a repetition rate of 10 Hz. With a stagnation pressure of 1.5 bar, the pressure in the source chamber does not exceed 3×10^{-6} Torr under operating conditions. The geometry of the discharge source is similar to that used by Van Beek *et al.* for the production of a pulsed beam of OH radicals [20]. To confine the discharge, a sharp-edged nozzle with an orifice of 0.5 mm diameter is used. A 0.5-mm diameter stainless steel ring with an inner diameter of 4.5 mm is mounted 2.5 mm in front of the nozzle. A voltage difference of 4.0 kV is applied between the ring and the valve body and can be pulsed using a fast high voltage switch (Behlke Electronic, HTS 61-03-GSM). The discharge has a duration of typically 10 μs. In the discharge, the NH molecules are produced in various electronic states, with only a fraction occupying the long-lived $a\,^1\Delta$ state. The quenching rate for the removal of NH molecules from this state by collisions with the He atoms is sufficiently low [21] that a beam of metastable NH can be produced. The beam passes through a 1.5-mm diameter skimmer and enters the detection chamber where the molecules can be state-selectively detected in a LIF zone 24 cm downstream from the nozzle. Here, a pulsed laser beam crosses the molecular beam at right angles. Laser induced fluorescence from this interaction region is spatially filtered and imaged on a photomultiplier tube (Electron Tubes B2/RFI, 9813 QB). A near-UV bandpass filter (Schott glass; UG11 filter) is used to block the ambient laboratory light. Stray light from the laser is reduced by using several 4-mm diameter light baffles. To reduce stray light further, the LIF optics are mounted inside a hollow, blackened stainless steel tube. Blackening of the surfaces is performed by growing a 10–20 μm thick copper film on the surfaces using electrolysis in a copper sulphate bath. A black copper-(II)oxide layer is formed when placing the product in a 100 °C bath containing sodium hydroxide and a strong oxidizer. The black surface attaches very well to the stainless steel and is, after baking, compatible with ultra-high vacuum applications ($\leqslant10^{-10}$ Torr), i.e., for future trapping experiments.

III. RESULTS AND DISCUSSION

A. Characterization of the molecular beam

To characterize the rotational state distribution of the metastable NH radicals in the molecular beam, the NH ($a\,^1\Delta$) radicals are detected by inducing the strong dipole allowed $c\,^1\Pi,v=0\leftarrow a\,^1\Delta,v=0$ transition around 326 nm. Pulsed laser radiation is generated by frequency-doubling the output of a Nd:YAG laser pumped dye laser system (Spectra Physics GCR-170/PDL3 combination) operating on DCM dye; typically some 10 mJ of tunable UV radiation with a bandwidth of 0.07 cm^{-1} is produced. In the experiment a pulse energy of only 0.5 mJ in a 4-mm diameter beam is used, sufficient to saturate the transition. Although the rotational levels in the $c\,^1\Pi,v=0$ state are predissociated, the lifetime is still around 460 ns and the total fluorescence quantum yield of these levels is about 90% [22,23]. Radiative decay from the $c\,^1\Pi,v=0$ state can occur via the $c\,^1\Pi\rightarrow b\,^1\Sigma^+$ and the $c\,^1\Pi\rightarrow a\,^1\Delta$ transitions. Only a few percent of the total fluorescence is in the $c\,^1\Pi\rightarrow b\,^1\Sigma^+$ channel around 450 nm [24], which is suppressed by the optical filter in our experiment. The observed $c\,^1\Pi\leftarrow a\,^1\Delta$ excitation spectrum is depicted in Fig. 1.

The observed lines are readily assigned using the line positions given by Ram *et al.* [25]. The ground rotational state $J=2$ is the most populated in the beam, but population of states up to $J=11$ is observed. The splitting of the lines due to the combined Λ-doublet splitting in the $c\,^1\Pi$ and the $a\,^1\Delta$ state is only resolved for high J-levels. Although no single rotational temperature can be fitted to the observed spectrum,

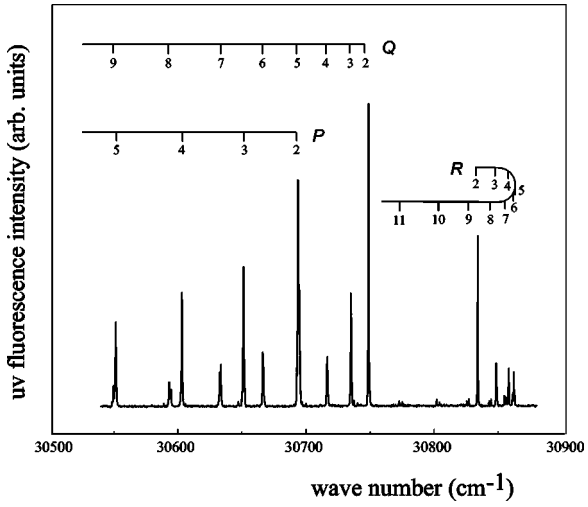

FIG. 1. The observed $c\,^1\Pi, v=0 \leftarrow a\,^1\Delta, v=0$ excitation spectrum for ^{14}NH, together with the assignment of the spectral lines.

a rotational temperature of about 120 K can be used to describe the relative population distribution of the lowest rotational levels. This relatively high rotational temperature is not unexpected in view of the limited cooling capacity of He in the expansion region combined with the hot discharge source. For the present study, the relatively wide rotational population distribution in the beam has the advantage that a rich $A\,^3\Pi \leftarrow a\,^1\Delta$ spectrum can be expected from which the relative rotational transition probabilities can be accurately determined.

From the observed LIF signals, an absolute number density for the NH radicals in one Λ-doublet component of the $a\,^1\Delta, v=0, J=2$ level of order 10^8 molecules/cm^3 is estimated. As the entrance of a decelerator will be closer to the source than the present LIF detection region, this value can be extrapolated to an anticipated number density of 10^9 molecules/cm^3 that can be accepted by a decelerator, and subsequently trapped. In successive experiments we have measured the population in the lowest rotational level in the metastable state and in the electronic ground state, i.e., the population in the $a\,^1\Delta, v=0, J=2$ level and in the $X\,^3\Sigma^-, v=0, N=0, J=1$ level. The latter is measured by recording (part of) the $A\,^3\Pi \leftarrow X\,^3\Sigma^-$ excitation spectrum around 336 nm. From these measurements it is deduced that with the present production method the population in the metastable state is about an order of magnitude less than the population in the electronic ground state.

B. The $A\,^3\Pi \leftarrow a\,^1\Delta$ transition

The spin-forbidden $A\,^3\Pi \leftarrow a\,^1\Delta$ transition around 584 nm is induced by the fundamental output of the same dye laser system, now operating on Rhodamine B dye. The radiative lifetime of the $A\,^3\Pi$ state is around 425 ns [26] and the far off-resonant $A\,^3\Pi \rightarrow X\,^3\Sigma^-$ fluorescence around 336 nm is collected in the LIF detection zone. Detection of the metastable NH radicals in this way is almost background-free as straylight from the laser beam is completely blocked by the optical filter. For the excitation, a 4-mm diameter laser beam with a pulse energy of typically 30 mJ in a 0.04 cm^{-1} bandwidth is used. Under these conditions the spin-forbidden transition is still not saturated, as will be discussed later. Absolute frequency calibration of the excitation laser is achieved by passing a reflection of the laser beam through an iodine absorption cell. The reported frequencies are corrected for systematic errors in the iodine reference atlas [27,28]. Measurements are performed for both ^{14}NH and ^{15}NH; the latter is produced from $^{15}NH_3$ (Campro Scientific; ^{15}N purity better than 99%).

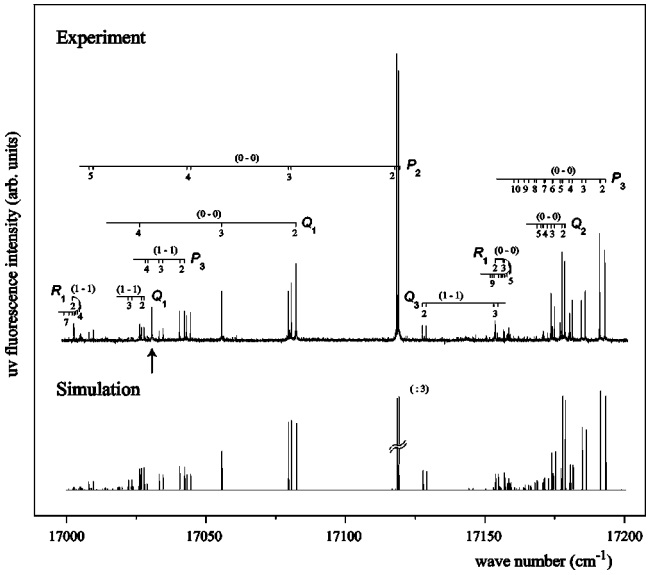

FIG. 2. Observed $A\,^3\Pi, v=0,1 \leftarrow a\,^1\Delta, v=0,1$ excitation spectrum of ^{14}NH together with the line assignment. The simulated spectrum, based on the spin-orbit coupling between the $A\,^3\Pi$ and $c\,^1\Pi$ states, is shown underneath. In the simulated spectrum, the intensity of the strong $P_2(2)$ line is reduced by a factor of 3. The line indicated with an arrow is due to metastable He atoms present in the beam.

The observed $A\,^3\Pi \leftarrow a\,^1\Delta$ excitation spectrum for ^{14}NH in the 17 000–17 200 cm^{-1} region is shown in Fig. 2. The spin-forbidden transition can gain intensity from the mixing of singlet character into the $A\,^3\Pi$ wave function. The latter can in principle occur via spin-orbit mixing of the $A\,^3\Pi$ state with the $a\,^1\Delta$, $b\,^1\Sigma^+$, or $c\,^1\Pi$ state. Only the $a\,^1\Delta$ and the $c\,^1\Pi$ state can contribute to the $A\,^3\Pi \leftarrow a\,^1\Delta$ transition intensity as the $b\,^1\Sigma^+ \leftarrow a\,^1\Delta$ transition is not electric dipole allowed. Since the spin-orbit coupling only connects levels with the same Ω quantum number, the $c\,^1\Pi$ state and the $a\,^1\Delta$ state only couple to the $\Omega=1$ and to the $\Omega=2$ components of the wave functions in the $A\,^3\Pi$ state, respectively. From the low $a\,^1\Delta \rightarrow X\,^3\Sigma^-$ spontaneous emission rate [15] the triplet character in the $a\,^1\Delta$ state is known to be low, and the $A\,^3\Pi - a\,^1\Delta$ coupling can be expected to be small. Therefore, the $A\,^3\Pi \leftarrow a\,^1\Delta$ excitation spectrum is simulated by taking exclusively the $A\,^3\Pi - c\,^1\Pi$ coupling into account. This simulated spectrum is shown underneath the observed spectrum in Fig. 2.

The spectral lines are assigned by using the molecular constants for $a\,^1\Delta$ and $A\,^3\Pi$ states given in the literature

[25,29,30]. The labelling of the lines is performed according to standard spectroscopic nomenclature. Using Hund's case (a) description, the three F_i manifolds in the inverted $A\,^3\Pi$ state are labeled F_1, F_2, and F_3 for $\Omega=2$, $\Omega=1$, and $\Omega=0$, respectively. This gives rise to nine branches in the $A\,^3\Pi_\Omega, J' \leftarrow a\,^1\Delta, J''$ transition which are denoted as $\Delta J_i(J'')$. The Q_1, R_1, P_2, Q_2, and the P_3 branch of the $v=0 \leftarrow v=0$ band are contained in the measured frequency range. Due to the Λ-doublet splitting in both electronic states, all lines in principle appear as doublets. The Λ-doublet splitting in the $a\,^1\Delta$ state is very small [30], and can be neglected in this study. The splitting of the lines as observed in the spectrum therefore directly reflects the Λ-doublet splitting in the $A\,^3\Pi$ state. The magnitude of this splitting strongly depends on the Ω character in the wave function of the specific rotational level involved.

For the simulation of the relative intensities of the spectral lines, the degree of $\Omega=1$ character in the wave function of the various rotational levels in the $A\,^3\Pi$ state has to be calculated. Since the ratio of the spin-orbit coupling constant to the rotational constant in the $A\,^3\Pi$ state is relatively small, this state rapidly approaches Hund's case (b) for higher rotational quantum numbers. Even for low values of J there is a large degree of Ω mixing, and a significant fraction of $\Omega=1$ character is present in the wave function of all rotational levels. The relative intensity of a $A\,^3\Pi_\Omega, J', e/f \leftarrow a\,^1\Delta, J'', e/f$ transition is simulated by multiplying the amount of $\Omega=1$ character in the wave function of the upper level with the Hönl-London factor of the corresponding dipole allowed $c\,^1\Pi, J' \leftarrow a\,^1\Delta, J''$ transition and with the population in the lower level. For the latter, the population distribution, as deduced from the experiments described in Sec. III A, is used.

As indicated in Fig. 2, a significant population in the $v=1$ level of the $a\,^1\Delta$ state is present. The $v=1 \leftarrow v=1$ band of the spin-forbidden transition is shifted some 150 cm^{-1} to the red, but several branches of this hot band appear in this same spectral region. The line observed at 17 030.59 cm^{-1} (indicated with an arrow) is not reproduced in the simulated spectrum. This line appears at the same frequency in the spectra of both ^{14}NH and ^{15}NH and can be assigned to the He($5\,^3D \leftarrow 2\,^3S$) two-photon transition, which is expected at exactly this frequency [31]. The long-lived metastable He($2\,^3S$) atoms are produced in the discharge source, and their spectral signature serves as an additional absolute frequency marker in our spectrum.

The correspondence between the observed and simulated spectrum is excellent, confirming that the $A\,^3\Pi \leftarrow a\,^1\Delta$ transition indeed mainly gains intensity due to $A\,^3\Pi - c\,^1\Pi$ spin-orbit coupling. Within the experimental accuracy no evidence for a $A\,^3\Pi - a\,^1\Delta$ coupling is found.

The measured and calculated line positions are given in Table I for both ^{14}NH and ^{15}NH for levels up to $J''=4$. The rotational constants for ^{15}NH are deduced from those of ^{14}NH using the isotope scaling laws. For each isotope and for both vibrational bands the $A\,^3\Pi - a\,^1\Delta$ singlet-triplet splitting is adjusted such that the calculated frequency of the most intense line, indicated in Table I, coincides with the observed line position. The overall agreement is excellent and apart from the singlet-triplet splitting for both isotopomers no adjustment of the spectroscopic constants is needed to fit the observed line positions.

As mentioned above, the measurements shown in Fig. 2 are taken under conditions away from saturation. In order to investigate the optical pumping efficiency from the $a\,^1\Delta$ state to the $X\,^3\Sigma^-$ ground state, experiments on the $A\,^3\Pi \leftarrow a\,^1\Delta$ transition have been performed with a narrow-band pulsed laser system with a superior spectral brightness. In this laser the output of a frequency stabilized single mode ring dye laser (Spectra Physics 380) is amplified in a three stage pulsed dye amplifier (Lambda Physik LPD 3000) pumped by a frequency-doubled injection seeded Nd:YAG pump laser (Spectra Physics GCR 190-50). Up to 80 mJ of 584 nm radiation is produced in a 5-ns duration pulse, with a Fourier transform limited bandwidth of approximately 90 MHz.

In view of the limited tunability of this laser system only the $A\,^3\Pi_1, v=0, J=1, e/f \leftarrow a\,^1\Delta, v=0, J=2, e/f$ transitions, the two strong components of the $P_2(2)$ doublet (see Fig. 2), are measured. The intrinsic shape of these lines is recorded using a pulse energy of 1 mJ in a 4-mm diameter beam, avoiding saturation broadening. The measured line profiles are shown for ^{14}NH in Fig. 3, and indicate unresolved hyperfine structure. Due to the nuclear spin of both N and H nucleus, the $a\,^1\Delta, J=2, e/f$ and $A\,^3\Pi_1, J=1, e/f$ Λ-doublet components are split into 6 (4) and 5 (4) hyperfine levels for ^{14}NH (^{15}NH), respectively. The hyperfine structure on the $A\,^3\Pi, v=0 \leftarrow X\,^3\Sigma^-, v=0$ transition and on the $c\,^1\Pi, v=0 \leftarrow a\,^1\Delta, v=0$ transition has been resolved and analyzed earlier [18,30]. Unfortunately, there are some mistakes in the formalism used in that analysis, which complicates the interpretation of the hyperfine interaction parameters presented in that work. We therefore reanalyzed the original data of Ubachs *et al.* [18,30] from which we calculated the expected hyperfine structure on the $P_2(2)$ line of the spin-forbidden transition. The transitions between the various hyperfine levels are indicated in Fig. 3 as a stick spectrum. The dashed curve is a convolution of the calculated spectrum with the spectral profile of the laser; for the latter a Gaussian distribution with a full width at half maximum of 90 MHz is assumed. There is an excellent match between the observed and expected line profiles. Equally good agreement is obtained for ^{15}NH (data not shown), when the reanalyzed hyperfine constants for ^{14}NH are isotopically scaled to ^{15}NH.

The absolute line frequencies for the two components of the $P_2(2)$ line as determined in these high resolution measurements, calibrated against the simultaneously measured iodine absorption spectrum, are incorporated in Table I. The tabulated experimental errors are deduced from the accuracy of the frequencies and the number of the individual iodine lines [27] that are used as frequency markers. The frequency of the $P_2(2)$ component that is most accurately measured in our experiments can be used to accurately determine the singlet-triplet splitting in NH. Together with the absolute frequencies of transitions in the $A\,^3\Pi, v=0 \leftarrow X\,^3\Sigma^-, v=0$ band [29], this yields a splitting between the lowest rovibrational level in the $X\,^3\Sigma^-$ state and the lowest rovibrational

TABLE I. Observed and simulated line positions (vacuum cm^{-1}) of the $A\,^3\Pi, v=0,1 \leftarrow a\,^1\Delta, v=0,1$ transition for ^{14}NH and ^{15}NH. The experimental error in the measured values is 0.03 cm^{-1}, unless stated otherwise. The deviation between measured and calculated values (observed-calculated) is given in parentheses. The lines that are used to determine the $A\,^3\Pi - a\,^1\Delta$ singlet-triplet splitting are indicated.

		^{14}NH				^{15}NH			
$^1\Delta, J, e/f$	line	$v=0 \leftarrow v=0$		$v=1 \leftarrow v=1$		$v=0 \leftarrow v=0$		$v=1 \leftarrow v=1$	
2, *e*	$Q_1(2)$	17082.01	(0.02)			17082.31	(0.01)		
	$R_1(2)$	17153.70	(−0.01)	17002.20	(0.01)	17153.75	(0.03)	17002.68	(0.00)
	$P_2(2)$	17117.993(2)	(fixed)			17118.315(10)	(fixed)		
	$Q_2(2)$	17178.53	(−0.01)	17027.23	(−0.01)	17178.57	(−0.01)	17027.73	(−0.03)
	$P_3(2)$	17191.02	(0.01)	17039.98	(0.02)	17191.08	(0.02)	17040.49	(0.00)
	$Q_3(2)$			17128.81	(0.00)			17128.94	(0.02)
2, *f*	$Q_1(2)$	17082.01	(0.02)			17082.31	(−0.01)		
	$R_1(2)$	17153.63	(0.01)	17002.13	(0.02)	17153.63	(−0.01)	17002.59	(−0.01)
	$P_2(2)$	17118.675(10)	(0.014)			17118.987(2)	(0.006)		
	$Q_2(2)$	17177.49	(0.00)	17026.25	(−0.01)	17177.53	(0.00)	17026.76	(−0.02)
	$P_3(2)$	17192.90	(0.01)	17041.78	(fixed)	17192.96	(0.01)	17042.31	(fixed)
	$Q_3(2)$			17127.49	(0.03)			17127.60	(0.03)
3, *e*	$Q_1(3)$	17055.13	(0.00)			17055.58	(0.00)		
	$R_1(3)$	17156.87	(−0.01)	17004.62	(0.00)	17156.90	(0.00)	17005.09	(−0.03)
	$P_2(3)$	17078.99	(0.00)			17079.47	(0.00)		
	$Q_2(3)$	17174.95	(0.02)	17022.91	(0.01)	17174.97	(−0.01)	17023.42	(0.00)
	$P_3(3)$	17184.52	(0.01)	17032.70	(0.03)	17184.56	(0.00)	17033.21	(0.00)
	$Q_3(3)$			17154.52	(0.00)			17154.50	(0.00)
3, *f*	$Q_1(3)$	17055.21	(0.00)			17055.66	(−0.01)		
	$R_1(3)$	17156.62	(−0.02)	17004.40	(0.01)	17156.64	(−0.02)	17004.90	(0.01)
	$P_2(3)$	17080.05	(0.00)			17080.52	(0.00)		
	$Q_2(3)$	17173.59	(−0.01)	17021.67	(0.02)	17173.65	(0.01)	17022.16	(−0.01)
	$P_3(3)$	17185.91	(0.02)	17034.01	(−0.01)	17185.95	(0.00)	17034.55	(−0.01)
	$Q_3(3)$			17153.56	(0.01)			17153.53	(0.00)
4, *e*	$Q_1(4)$	17025.49	(−0.01)			17026.09	(−0.02)		
	$R_1(4)$	17158.46	(−0.02)	17005.19	(0.01)	17158.51	(0.01)	17005.72	(0.01)
	$P_2(4)$	17042.45	(−0.01)			17043.07	(−0.02)		
	$Q_2(4)$	17172.42	(−0.01)			17172.46	(−0.02)		
	$P_3(4)$	17180.25	(0.01)	17027.34	(−0.01)	17180.31	(0.01)	17027.88	(−0.01)
	$Q_3(4)$			17180.76	(0.01)			17180.02	(0.03)
4, *f*	$Q_1(4)$	17025.72	(−0.02)			17026.34	(−0.01)		
	$R_1(4)$	17157.98	(−0.02)	17004.77	(0.02)	17158.02	(0.00)	17005.27	(0.01)
	$P_2(4)$	17043.79	(0.00)			17044.41	(−0.02)		
	$Q_2(4)$	17170.80	(−0.01)			17170.86	(0.00)		
	$P_3(4)$	17181.22	(−0.01)	17028.31	(−0.01)	17181.30	(0.01)	17028.85	(−0.01)
	$Q_3(4)$			17180.16	(0.02)			17180.02	(0.03)

level in the $a\,^1\Delta$ state for ^{14}NH of 12 688.622 ± 0.004 cm^{-1}. From a direct measurement of the $a\,^1\Delta, v=0, J=2 \rightarrow X\,^3\Sigma^-, v=0, N=0, J=1$ transition, this singlet-triplet splitting has previously been reported to be 12 687.8 ± 0.1 cm^{-1} [15]. The inaccurate frequency calibration method used in those experiments probably explains the discrepancy with the value determined in our measurements.

By increasing the pulse energy of the narrow-band pulsed dye laser system, the $P_2(2)$ line of the spin-forbidden transition can be saturated; with 10 mJ in a 4-mm diameter beam saturation effects are already observed. This leads to an order of magnitude estimate for the peak absorption cross section for this transition of 10^{-18} cm^2, corresponding to a value of the Einstein *A*-coefficient of order unity. In a previous paper we calculated, taking exclusively the $^3\Pi - {}^1\Pi$ interaction into account, the transition dipole moment for the $P_2(2)$ transition would be around 4.4×10^{-4} atomic units (a.u.) [10], in good agreement with the present findings of about 5×10^{-4} atomic units. In the accumulation scheme discussed earlier, the NH radicals are optically pumped to their electronic ground state at a point where the molecules have come to a near standstill. The strength of the spin-forbidden transition in NH suggests that in this case it will even be possible to achieve efficient optical pumping from the metastable

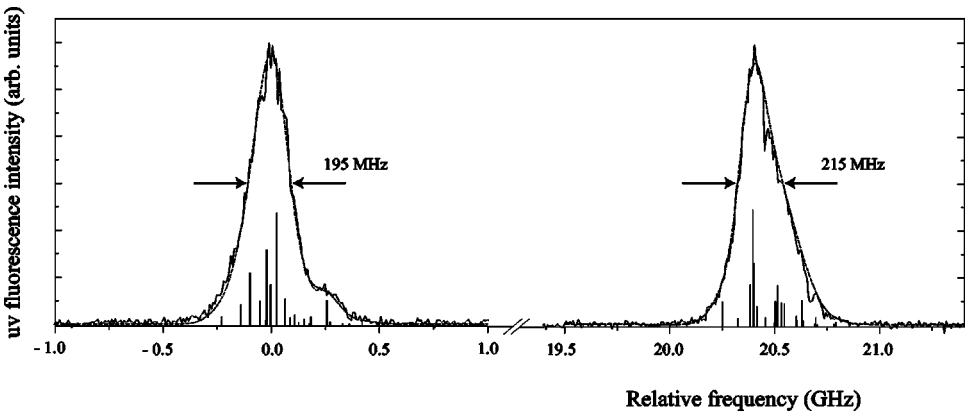

FIG. 3. The $A\,^3\Pi \leftarrow a\,^1\Delta, P_2(2)$ transitions for ^{14}NH, measured with a 90-MHz bandwidth pulsed dye laser system. The calculated transitions between the various hyperfine levels are given as a stick spectrum. The dashed curve is the convolution of the stick spectrum with the spectral profile of the laser.

state to the electronic ground state using a cw laser system. This allows optical pumping from selected hyperfine levels, and enables the production of trapped molecules that occupy only a limited, and well-defined, number of hyperfine levels.

IV. CONCLUSIONS

An intense pulsed molecular beam of metastable NH ($a\,^1\Delta$) radicals is produced and characterized. By inducing the hitherto unobserved spin-forbidden $A\,^3\Pi \leftarrow a\,^1\Delta$ transition, efficient optical pumping of the metastable radicals to their electronic ground state is demonstrated. The expected mechanism via which this transition gains intensity is verified, and the absolute transition probability is estimated from the experimental data. The optical pumping scheme opens up the possibility to accumulate the NH radicals in a trap. It is remarked that the $A\,^3\Pi \leftarrow a\,^1\Delta$ transition characterized in this work allows the complete background free detection of metastable NH radicals; although the use of a spin-forbidden transition for LIF detection of molecules is unconventional, it might actually be the most sensitive method to detect metastable NH radicals.

ACKNOWLEDGMENTS

This work is part of the research program of the ''Stichting voor Fundamenteel Onderzoek der Materie (FOM),'' which is financially supported by the ''Nederlandse Organisatie voor Wetenschappelijk Onderzoek (NWO).'' The research of R.T.J. was sponsored by the Royal Netherlands Academy of Arts and Sciences. We thank P. H. M. Smeets for expert technical support.

[1] J.T. Bahns, P. Gould, and W.C. Stwalley, Adv. At., Mol., Opt. Phys. **42**, 171 (2000).
[2] F. Masnou-Seeuws and P. Pillet, Adv. At., Mol., Opt. Phys. **47**, 53 (2001).
[3] H.L. Bethlem and G. Meijer, Int. Rev. Phys. Chem. **22**, 73 (2003).
[4] N. Vanhaecke, W. de Souza Melo, B.L. Tolra, D. Comparat, and P. Pillet, Phys. Rev. Lett. **89**, 063001 (2002).
[5] J.D. Weinstein, R. deCarvalho, T. Guillet, B. Friedrich, and J.M. Doyle, Nature (London) **395**, 148 (1998).
[6] H.L. Bethlem, G. Berden, F.M.H. Crompvoets, R.T. Jongma, A.J.A. van Roij, and G. Meijer, Nature (London) **406**, 491 (2000).
[7] F.M.H. Crompvoets, H.L. Bethlem, R.T. Jongma, and G. Meijer, Nature (London) **411**, 174 (2001).
[8] H.L. Bethlem, F.M.H. Crompvoets, R.T. Jongma, S.Y.T. van de Meerakker, and G. Meijer, Phys. Rev. A **65**, 053416 (2002).
[9] M. Baranov, L. Dobrek, K. Goral, L. Santos, and M. Lewenstein, Phys. Scr., T **102**, 74 (2002).
[10] S.Y.T. van de Meerakker, R.T. Jongma, H.L. Bethlem, and G. Meijer, Phys. Rev. A **64**, 041401(R) (2001).
[11] D.R. Yarkony, J. Chem. Phys. **91**, 4745 (1989).
[12] P.W. Fairchild, G.P. Smith, D.R. Crosley, and J.B. Jeffries, Chem. Phys. Lett. **107**, 181 (1984).
[13] W. Hack, *N-Centered Radicals* (Wiley, New York, 1998), Chap. 13, pp. 413–466.
[14] A. Gilles, J. Masanet, and C. Vermeil, Chem. Phys. Lett. **25**, 346 (1974).
[15] J.L. Rinnenthal and K.-H. Gericke, J. Mol. Spectrosc. **198**, 115 (1999).
[16] D. Patel-Misra and P.J. Dagdigian, J. Chem. Phys. **97**, 4871 (1992).
[17] D.G. Sauder, D. Patel-Misra, and P.J. Dagdigian, J. Chem. Phys. **91**, 5316 (1989).
[18] W. Ubachs, J.J. ter Meulen, and A. Dymanus, Can. J. Phys. **62**, 1374 (1984).
[19] Y. Mo, C. Ottinger, and G. Shen, J. Chem. Phys. **111**, 4598 (1999).
[20] M.C. van Beek and J.J. ter Meulen, Chem. Phys. Lett. **337**, 237 (2001).
[21] R.D. Bower, M.T. Jacoby, and J.A. Blauer, J. Chem. Phys. **86**, 1954 (1987).
[22] B. Bohn, F. Stuhl, G. Parlant, P.J. Dagdigian, and D.R. Yarkony, J. Chem. Phys. **96**, 5059 (1992).
[23] G. Parlant, P.J. Dagdigian, and D.R. Yarkony, J. Chem. Phys. **94**, 2364 (1991).
[24] W. Hack and T. Mill, J. Phys. Chem. **97**, 5599 (1993).
[25] R.S. Ram and P.F. Bernath, J. Opt. Soc. Am. B **3**, 1170 (1986).

[26] R.D. Kenner, A. Kaes, R.K. Browarzik, and F. Stuhl, J. Chem. Phys. **91**, 1440 (1989).
[27] S. Gerstenkorn and P. Luc, *Atlas du spectroscopie d'absorption de la molecule d'iode* (CNRS, Paris, 1978).
[28] S. Gerstenkorn and P. Luc, Rev. Phys. Appl. **14**, 791 (1979).
[29] C.R. Brazier, R.S. Ram, and P.F. Bernath, J. Mol. Spectrosc. **120**, 381 (1986).
[30] W. Ubachs, G. Meijer, J.J. ter Meulen, and A. Dymanus, J. Mol. Spectrosc. **115**, 88 (1986).
[31] W.C. Martin, Phys. Rev. A **36**, 3575 (1987).